Fenton coupled with nanofiltration for elimination of Bisphenol A

I. Escalona[a], A. Fortuny[b], F. Stüber[a], C. Bengoa[a], A. Fabregat[a], J. Font[a]

[a]Departament d'Enginyeria Química, ETSEQ, Universitat Rovira i Virgili, Av. Països Catalans 26, 43007 Tarragona, Spain.
(E-mail: ivonne.escalona@urv.cat, frankerich.stuber@urv.cat, christophe.bengoa@urv.cat, afabrega@urv.cat, jose.font@urv.cat)

[b]Departament d'Enginyeria Química, EPSEVG, Universitat Politècnica de Catalunya, Av. Víctor Balaguer, s/n, 08800 Vilanova i la Geltrú, Spain.
(E-mail: agustin.fortuny@upc.es)

Abstract

Bisphenol A (BPA) is a typical Endocrine Disrupting Chemical (EDC), which is potentially harmful during wastewater reclamation. In this study, its degradation during Fenton's process under different operational conditions was investigated in combination with subsequent nanofiltration of low concentration remnant BPA and compounds derived from oxidation. The results indicate that BPA could be degraded efficiently in aqueous phase by Fenton, even at very low hydrogen peroxide doses. The treatment of up to 300 mg/L solutions of BPA with Fenton liquor at optimal conditions resulted in its complete removal in less than 2 min. The optimal conditions were found to be pH_r = 3, H_2O_2/BPA = 0.20 and Fe^{2+}/BPA = 0.012. Five NF polymeric membranes having different properties were used for the nanofiltration of treated and non-treated solutions. The nanofiltration of BPA solutions showed that rejection is related to adsorption ability of BPA on the membrane and size exclusion mechanism. In the nanofiltration of the effluent after Fenton oxidation, high TOC, COD, colour and Fe^{2+} (>77%) removal were achieved, although significant membrane fouling was also observed. The normalised water flux after membrane flushing with water was lower than 60% in almost all used membranes, which indicates significant non-easily removable fouling.

Keywords: nanofiltration; BPA removal; Fenton process; water treatment.

1. INTRODUCTION

Various adverse health effects of endocrine disrupting compounds (EDCs) have been reported in recent years [1, 2]. Bisphenol A (BPA) is a representative endocrine disrupter. It has been widely used as the monomer for the production of polycarbonate plastics and as a major component of epoxy resin [3]. BPA has been detected in all kinds of environmental water, not only found in industrial wastewater, but also can be encountered in raw water [4]. The maximum concentrations reached up to 17.2 mg/L in hazardous waste landfill leached [5], but appears at low concentrations in many other effluents, e.g., 12 μg/L in stream water [6] and 0.1 μg/L in drinking water [7], although it can be detected at much higher level, even several hundreds of mg/L, in specific industrial emitters [8]. It is reported that BPA exhibited estrogenic activity [9], which increases the rate of proliferation of breast cancer cells and induces acute toxicity to freshwater and marine species [10], at a low dose of 0.23 pg/mL culture medium [3]. Therefore, the development of treatment techniques for the decomposition and removal of BPA in water is urgently required.

BPA can indeed be degraded by microorganisms. However, it is hard to be completely eliminated by conventional biological treatment method [11], which inevitably leads to the existence of residual BPA in aqueous solution, so its removal should often be addressed at the source, before the effluent is driven to a wastewater treatment plant (WWTP). Various methods have been developed to remove BPA from water, such as biological methods [12-14], chemical oxidation [14], electrochemical oxidation [15], and photocatalytic methods [16, 17]. Due to the role of highly reactive free radicals, Advanced Oxidation Processes (AOPs) have shown the ability to destructively oxidize BPA from sewage and water. Recent studies on chemical oxidation by ozone [18], UV photolysis [19], UV/H_2O_2 [20], photo-Fenton process [21] and TiO_2 photocatalysis [16] have shown the usefulness of AOPs for removing BPA.

The Fenton treatment, as AOP, can be an effective way to treat water and remove micropollutants such as BPA. The simple principle of the Fenton process is the catalytic cycle of the reaction between iron salts (catalyst) and hydrogen peroxide (oxidant) to produce hydroxyl radicals (•OH). These radicals are very effective to degrade organic pollutants because of their strong oxidant power.

Fenton's reagent is particularly attractive because of the low cost, the lack of toxicity of the reagents (i.e., Fe^{2+} and H_2O_2), the absence of mass transfer limitation due to its homogeneous catalytic nature and the simplicity of the technology required [22], while other AOPs have high demand of electrical energy for devices such as ozonators, UV lamps, ultrasounds, etc., and this makes them economically disadvantageous. However, since Fenton process requires ferrous salt for the oxidation reaction to take place, the iron hydroxide sludge formed after the reaction has to be removed before discharging.

Studies of the degradation of BPA by AOPs, such as Fenton, during water treatment are still scarce. The application of nanofiltration (NF), as promising membrane technology, could be an alternative method for removing and concentrating low molecular weight organic micropollutants. There have been numerous attempts to enhance oxidation with additional process steps. In this case, membrane separation is becoming a very attractive alternative because of its purely physical nature of separation as well as the modular design of membrane processes [23]. Among many others, separation without phase change, low energy consumption, and operability at ambient temperature have given an edge to membrane processes over the conventional processes. Therefore, NF has a potential applicability in Fenton process as catalyst remover, in order to reduce the iron concentration in wastewater before discharge and avoid the subsequent separation of iron hydroxide sludge. Additionally, the combination of Fenton process and NF allows recycling of the soluble iron to the reaction tank for reuse during the process of BPA degradation, which also reduces the continuous addition of catalyst as well as decreases treatment cost.

Thus, considering the widespread detection of BPA in the environment and the limited data available in the literature on the treatment of BPA contaminated water, the main objective of this study was to investigate the degradation of BPA during Fenton's process under different operational conditions, which was combined with NF of the treated effluent containing low concentration remnant BPA and derived partial oxidation intermediates. In this sense, efficiency of the removal BPA and oxidation intermediates by the NF was also evaluated through several polymeric membranes.

2. MATERIALS AND METHODS

2.1 Materials and reagents

All chemicals were obtained in analytical grade. BPA was purchased from Sigma-Aldrich (USA); some properties are shown in Table 1. Deionised water was used to prepare all the solutions. Hydrogen peroxide was supplied by Panreac (Spain) as a 30% w/v aqueous solution. For Fenton experiments, Fe^{2+} salt used as catalyst was ferrous sulphate 7-hydrate ($FeSO_4 \cdot 7H_2O$); it was obtained from Panreac at 99% purity.

Because of its commercial availability and successful application on different cases, five standard polymeric NF membranes, i.e., NFD, NF90, NF270 (Dow Filmtec, USA), ESNA1-LF2 (Hydranautics, USA) and CK (GE Osmosnics, USA) were used for studying the potential of NF over BPA and partial oxidation products. These names correspond to the commercial designations with the exception of NFD. NFD is commercially designated as NF but, for avoiding confusions with the universally accepted acronym for nanofiltration, NF, this membrane is named NFD throughout the text. Moreover, ESNA1-LF2 was abbreviated as ESNA. Table 2 gives the most important properties of the selected membranes.

Table 1. BPA properties [12, 24, 25].

Properties	**Data**
Chemical name	2.2-(4.4-dihydroxydiphenyl) propane
Molecular structure	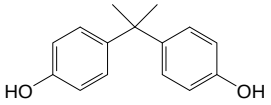
Formula	$C_{15}H_{16}O_2$
Molecular Weight	228.28
Specific gravity at 25 ºC, (g/cm^3)	1.06
Octanol-water partition coefficient	3.32
pK_a	9.6 to10.2
Water solubility, (mg/L)	120-300
Molecular size (nm)	Molecular width X: 0.383
	Molecular width Y: 0.587
	Molecular width Z: 1.068

Table 2. Properties of the polymeric membranes tested.

Membrane name	Isoelectric point (pH)	Pore radius (nm)	MWCO (Da)	PWP[(a)] (L/m^2 h bar)	Active layer[(b)]	Roughness[(c)] (nm)	Contact angle (º)	Ref.
NFD	5.1	-	≤200	8.17 ± 0.46	semi-aromatic piperazine-based polyamide TFC	0.16	-	[26, 27]
NF90	4	0.34	200	10.97 ± 0.37	polyamide TFC	57.23	42	[28]
NF270	3.5	0.42	300	14.44 ± 0.80	semi-aromatic piperazine-based polyamide TFC	4.47	30	[28,29]
CK	-	-	150-300	1.56 ± 0.02	Cellulose Acetate	8.36	54	[30]
ESNA	4.9	-	100-300	9.69 ± 1.09	meta-phenylene diamine-based polyamide	60.68	60	[26, 31]

[(a)] Pure Water Permeability, PWP, was experimentally measured.

[(b)] All the membranes use polysulphone as support layer.

[(c)] Roughness was determined from AFM images using WSxM v5.0 Develop 6.2 software.

2.2 Fenton experiments

Appropriate amounts of BPA solution and ferrous salt were added to a beaker and diluted with deionised water up to 1 L. The Fenton reaction was done in a water-jacketed glass reactor. The reactor was filled with 1 L of BPA and ferrous salt solution at different BPA concentrations, 13 to 300 mg/L, and Fe^{2+}/H_2O_2 molar ratio, 0.0 to 0.1. As iron hydrolysis rate was found to affect Fenton process efficiency [32], the BPA and ferrous salt solutions were immediately used after their preparation. Then the initial pH was measured and, in some cases, adjusted at 3 using HCl 2 mol/L since, according to literature [33], it is the optimum pH to promote the generation of hydroxyl radicals in Fenton process. The reaction time was considered to start when hydrogen peroxide was added. The H_2O_2/BPA stoichiometric molar ratio was tested in the range from 0.05 to 1.00.

Samples (5 mL) were periodically withdrawn for analysis and placed in the refrigerator at 4 ± 1 ºC or basified at pH 11-12 with NaOH 2 mol/L to stop the reaction. When the reaction solution was prepared with the aim of testing the efficiency of the subsequent membrane treatment, basification was not used because the nature of the solution would change, affecting the filtration efficiency and thus the reliability of the filtration results. Basification was only applied in samples for Chemical Oxygen Demand (COD) measurements since residual H_2O_2 is known to affect COD determination [34].

Overall, the effect of different system variables, namely Fe^{2+}/H_2O_2 and H_2O_2/BPA molar ratio, initial BPA concentration and reaction time were studied. All experiments were conducted at controlled temperature (T_r = 30 ± 1 ºC) and at a stirring rate of 300 rpm for a time reaction, t_r, up to 120 min. Full mineralisation of BPA is given by eq. 1. This equation was used to normalise the oxidant to BPA molar ratio, i.e. H_2O_2/BPA stoichiometric molar ratio equal to 1 represents the addition of stoichiometric amounts of the reagents (1 mol of BPA and 36 mol of H_2O_2).

$$C_{15}H_{16}O_2 + 36H_2O_2 \rightarrow 15CO_2 + 44H_2O \qquad \text{(eq. 1)}$$

2.3 Nanofiltration system and tests

BPA solution and BPA effluent after Fenton degradation at selected optimal oxidation conditions were filtered in a NF cell. The equipment was a home-made cross flow lab scale plant. It includes a cross flow cell, a feed pump, 1 L reservoir tank, a pressure dampener and pressure gauges to control pressure along the experiment. Full recirculation mode was used during the experiment, where both retentate and permeate were returned to the feed tank in order to maintain constant concentration at controlled temperature (T_f = 30 ± 1 ºC). Permeate was collected at atmospheric pressure. The effective membrane surface was 42 cm^2 and the entering flow rate, Q_f, was 20 L/h. A scheme of the system is depicted in Figure 1.

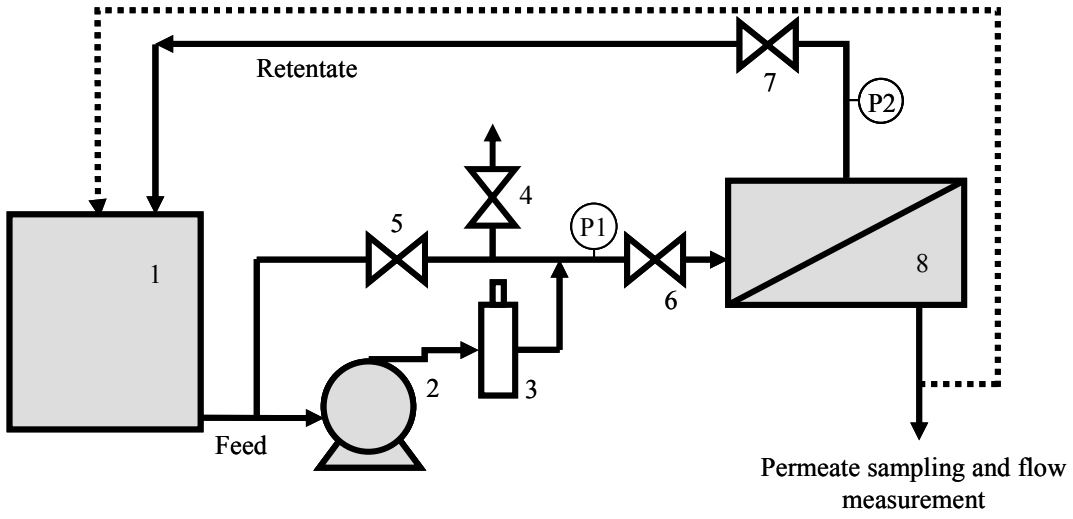

Figure 1. Filtration experimental set-up. (1) Feed tank, (2) pump, (3) pulse dampener, (4) relief valve, (5) bypass valve, (6) and (7) backpressure valves, (8) membrane cell, (P1) and (P2) pressure gauges.

As membrane preconditioning can influence its further performance, prior to use, each membrane was immersed in deionised water for 24 h to ensure the complete removal of any impurity and its hydration. Later, the membrane was compacted for at least 1 hour using deionised water at 8 bar. Pure water permeability was then determined at the end of the compaction process. A typical test started by filling up the feed tank with 1 L of solution and putting the system at specified operational conditions. Permeate and feed samples were collected for analysis at given intervals. After a filtration run, pure water flux was measured again using deionised water in order to know the permeate flux decrease and membrane fouling due to filtration. The effect of membrane type, initial concentration, and transmembrane pressure on permeate flux were studied.

Membrane efficiency was determined using the ratio between actual permeate flux, J_p, and pure water permeate flux of the clean membrane, J_{w0}, and the rejection, R, expressed by Eq. 2:

$$R(\%) = 100.\frac{C_f - C_p}{C_f} \qquad \text{(eq. 2)}$$

where C_f and C_p are the solute concentration of the feed and the permeate, respectively.
The J_p/J_{w0} ratio is known as normalised permeate flux and is also a measure of the permeate flux decline during filtration.

To evaluate the repeatability in the NF experiments, an arithmetic mean was calculated from three well-reproduced repetitions of BPA filtration at 300 mg/L, 6 bar and 30 ºC using NF90 membrane. The difference between data and their corresponding arithmetic means was less than 5 and 13% for normalised fluxes and BPA rejections, respectively, which are values typically occurring in membrane performance tests.

2.4 Analysis methods

BPA concentration was determined by high-performance liquid chromatography (Agilent Series 1100-Germany) using a C18 reverse phase column (Tracer Extrasil ODS-2, 5 µm, 25 x 0.4 cm-Germany). A methanol/water mixture (55/45 v/v) was used as the mobile phase with a flow-rate of 1 mL/min. For each sample, the injected volume was 200 µL. Column effluent

was monitored with UV-visible spectrometer at 270 nm. For Total Organic Carbon (TOC), analysis was conducted in an Analytic Jena TOC Analyzer (model multi N/C 2100, Germany). COD in the samples was analysed by the closed reflux colorimetric standard method 5220D [35]. Finally, colour in oxidised Fenton effluents was measured by absorbance (Abs) reading in the visible range using an UV-VIS spectrophotometer (Dinko, model 8500, Spain). A wavelength scan was carried out and the wavelength corresponding to the maximum absorbance was selected for assessing the colour of the samples.

3. RESULTS AND DISCUSSION

3.1 Fenton degradation of BPA

The oxidation tests were carried out in a 1 L batch reactor using hydrogen peroxide as oxidizing agent and iron (II) sulphate heptahydrate as catalyzing agent (Fenton reagent) at 30 (± 1) ºC and pH_r = 3.00 (±0.01) for 120 min. Table 3 summarises the operating conditions in terms of BPA initial concentration, H_2O_2/BPA stoichiometric molar ratio and Fe^{2+}/H_2O_2 molar ratio. Sub-stoichiometric amounts of H_2O_2 oxidant were used to simulate economically viable processes and operation under not fully controlled conditions. Although Fenton reaction has been widely studied, the optimal Fe^{2+}/H_2O_2 ratio differs. In the present study, the optimal ratio was considered to be 0.012, below the theoretical optimum ratio of 0.091 reported in previous studies [36, 37].

Table 3 shows the effect of BPA concentration on the final conversion of BPA (X_fBPA) by Fenton. The increase of BPA concentration from 100 to 300 mg/L only decreases the conversion in 13.7%. The hydroxyl radicals are mainly responsible for BPA degradation and its concentration is assumed to remain similar for all BPA concentrations, since H_2O_2 and Fe^{2+} initial concentration used were constant. The increase in BPA concentration increases the number of BPA molecules to be degraded whereas the hydroxyl radical availability is essentially maintained, so the degradation level decreases. This behaviour is corroborated observing the decrease in final conversion of COD (X_fCOD) and TOC (X_fTOC) from 38.3 to 11.9% and from 16.8 to 3.3%, respectively. At BPA concentration below 100 mg/L, maximum BPA conversion was observed. However, it also resulted in a decrease of the X_fCOD and X_fTOC. This behaviour indicates that, at high hydrogen peroxide doses, H_2O_2/BPA > 1.12, parasitic reactions are favoured, where oxidative radicals are scavenged by

partial oxidation products and/or self-consumed, yielding a decrease of the oxidation efficiency.

Table 3. Effect of BPA initial concentration, and H_2O_2/BPA and Fe^{2+}/H_2O_2 initial molar ratios on the conversion and colour after 120 min oxidation. Conditions: T_r = 30 ºC, t_r = 120 min, pH_r = 3 and 300 rpm.

[BPA] (mg/L)	**[H_2O_2] (mg/L)**	**[Fe^{2+}] (mg/L)**	**H_2O_2/BPA**	**Fe^{2+}/H_2O_2**	***X_f*BPA (%)**	***X_f*COD (%)**	***X_f*TOC (%)**	**Abs (400 nm)**	**pH_f**
13	150	3	2.23	0.012	100 ± 2.1	19.5 ± 1.0	11.4 ± 0.9	0.020	2.94
25	150	3	1.12	0.012	100 ± 2.8	22.4 ± 2.3	14.7 ± 0.1	0.038	2.91
50	150	3	0.56	0.012	100 ± 2.2	45.3 ± 2.1	36.9 ± 0.6	0.120	2.84
100	150	3	0.28	0.012	100 ± 2.1	38.3 ± 0.2	16.8 ± 0.8	0.192	2.81
200	150	3	0.14	0.012	97.5 ± 2.1	19.1 ± 1.3	7.3 ± 0.9	0.324	2.81
300	150	3	0.09	0.012	86.3 ± 2.0	11.9 ± 0.1	3.3 ± 0.1	0.325	2.83
300	75	1	0.05	0.012	57.5 ± 1.9	37.8 ± 0.2	16.5 ± 0.5	0.325	2.98
300	159	3	0.10	0.012	85.5 ± 1.8	26.6 ± 0.1	13.8 ± 0.8	0.392	2.80
300	242	5	0.15	0.012	97.9 ± 1.8	35.5 ± 1.8	16.5 ± 0.6	0.580	2.81
300	323	6	0.20	0.012	99.7 ± 1.8	44.6 ± 2.1	26.1 ± 0.8	0.652	2.71
300	644	13	0.40	0.012	99.8 ± 1.8	66.1 ± 2.2	29.5 ± 0.6	0.267	2.54
300	1608	31	1.00	0.012	100 ± 1.2	78.2 ± 1.3	59.1± 0.6	0.106	2.45
300	323	0	0.20	0.000	19.8 ± 1.4	6.7 ± 1.6	3.7 ± 0.6	0.026	2.97
300	323	2	0.20	0.003	93.3 ± 1.7	24.8 ± 1.7	19.9 ± 0.6	0.697	2.80
300	323	3	0.20	0.006	94.8 ± 1.7	25.0 ± 1.9	19.6 ± 0.6	0.696	2.77
300	323	26	0.20	0.050	97.8 ± 1.1	23.6± 1.8	13.9± 0.3	0.743	2.72
300	323	52	0.20	0.100	98.4 ± 1.2	23.8 ± 1.6	14.3 ± 0.7	0.756	2.79

Figure 2 presents the temporal evolution of BPA conversion for 100, 200 and 300 mg/L of initial concentration of BPA. The maximum conversions were immediately reached upon initiation of the reaction. The rapid degradation of BPA is believed to be due to the higher efficiency for the production of large amount of hydroxyl radicals by the reaction of ferrous ions with H_2O_2 and the high reactivity of BPA with these hydroxyl radicals.

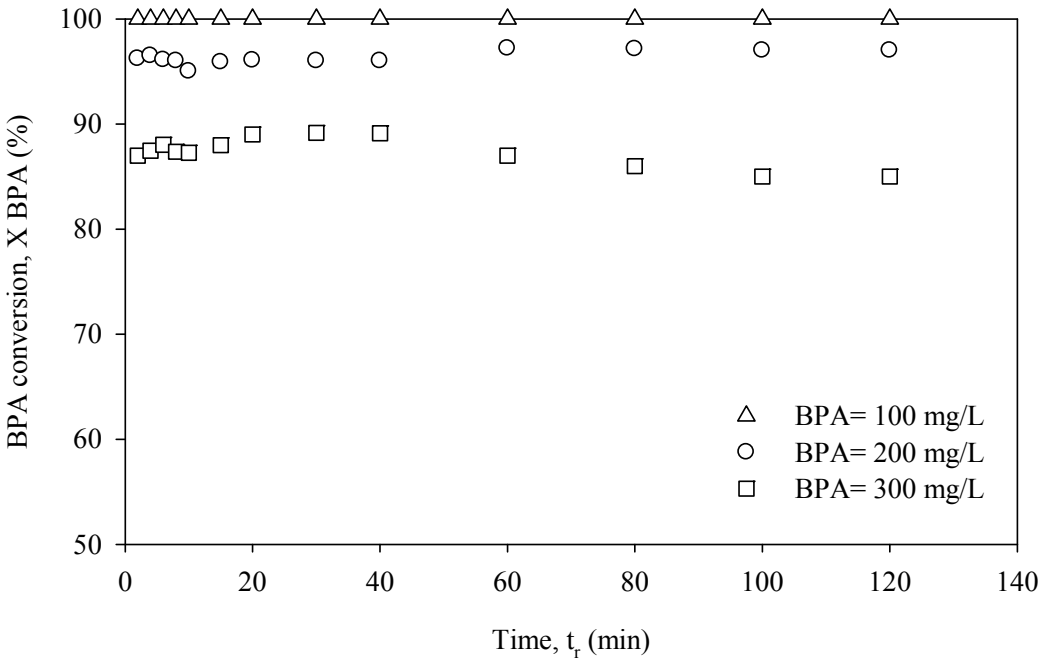

Figure 2. BPA conversion as a function of reaction time for several BPA initial concentrations. Conditions: $[Fe^{+2}]$ = 3 mg/L; $[H_2O_2]$ =150 mg/L; pH_r = 3; T_r = 30 ^oC, and 300 rpm.

The effect of H_2O_2/BPA stoichiometric molar ratio on the Fenton process is also shown in Table 3 and Figure 3. In those experiments, a Fe^{2+}/H_2O_2 molar ratio and a BPA initial concentration of 0.012 and 300 mg/L were chosen, respectively. Altogether, an increase in the H_2O_2/BPA stoichiometric molar ratio was positive for the degradation of BPA in all the studied range. The BPA degradation efficiency was better when increasing the H_2O_2/BPA ratio in the range from 0.05 to 0.15. BPA conversion increased from 57.7 to 97.9%. This behaviour could be due to the improved oxidation power with increasing hydroxyl radical amounts in the solution generated from H_2O_2. For H_2O_2/BPA above 0.20, the BPA conversion kept constant, however X_fCOD and X_fTOC continuously increased. X_fCOD increased from 44.6 to 78.2% and X_fTOC from 26.1 to 59.1%. This was due to the deeper degradation of the oxidation intermediates. Furthermore, the increase in the X_fCOD as a function of H_2O_2/BPA stoichiometric molar ratio in all the studied range can be explained by the generation of by-products with lower number of carbons atoms in their structures, which required less oxygen for their chemical oxidation and compete for the oxyradicals.

It is worth mentioning that, in spite of the use of the stoichiometric amount required (H_2O_2/BPA=1), complete mineralisation of BPA was not observed, as evidenced by the

59.1% in the X_fTOC obtained at this condition. In general, the maximum conversions were reached before 15 min of the reaction as it is shown in Figure 3.

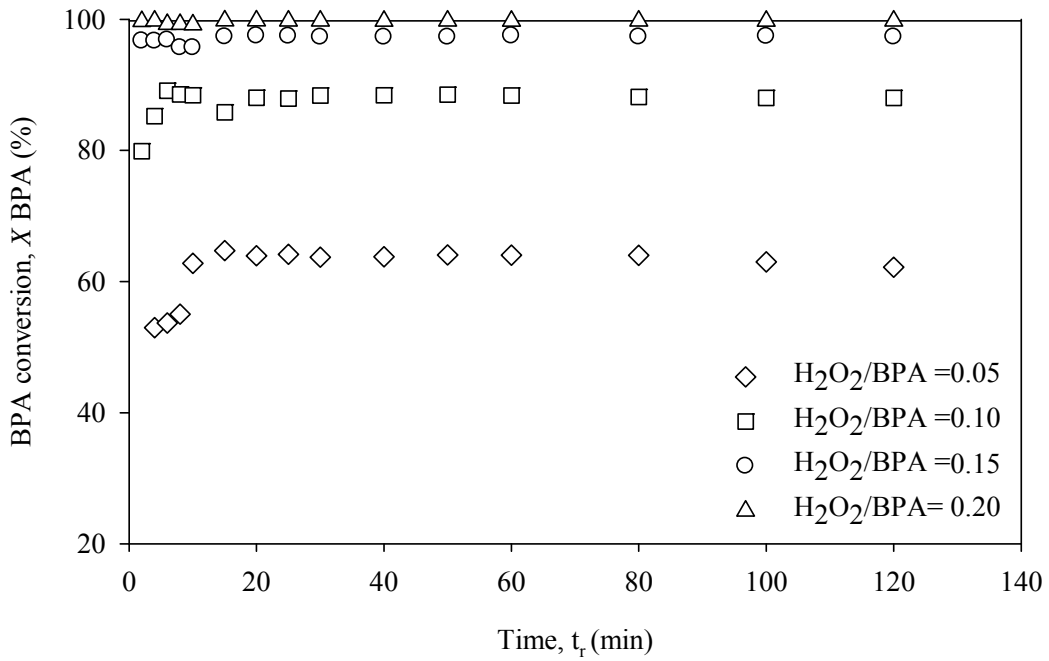

Figure 3. BPA conversion as a function of reaction time for several H_2O_2/BPA stoichiometric molar ratios. Conditions: [BPA] = 300 mg/L; Fe^{+2}/H_2O_2 = 0.012; pH_r = 3; T_r = 30 °C and 300 rpm.

To find out the optimal iron load, several experiments were performed by increasing the catalyst concentration, while maintaining the initial BPA concentration, H_2O_2/BPA stoichiometric molar ratio and reaction time at 300 mg/L, 0.18 and 120 min, respectively. The BPA underwent 97% degradation under most experimental conditions (Table 3). A Fe^{2+}/H_2O_2 ratio as low as 0.003 already gave a BPA degradation of 93.3%. As expected, the increase on the iron load increases the production rate of hydroxyl radicals, which leads to a higher effluent mineralisation. However, beyond Fe^{2+}/H_2O_2 = 0.003, the X_fCOD and X_fTOC remained almost constant despite the increasing doses of Fe^{2+} applied. Thus, the use of a too high Fe^{2+} concentration could lead to the self-scavenging of hydroxyl radicals by Fe^{2+} and induce the stabilization or even decrease of the degradation of pollutants. It was also observed that, in the absence of Fe^{2+}, there was degradation, yet low, indicating that H_2O_2 can react with BPA without need of any catalyst. Hence, in the range studied, it was possible to conclude that high iron load had not much impact on BPA degradation during Fenton's treatment. The degradation of BPA as a function of the reaction time for several Fe^{2+}/H_2O_2 molar ratio is shown in Figure 4.

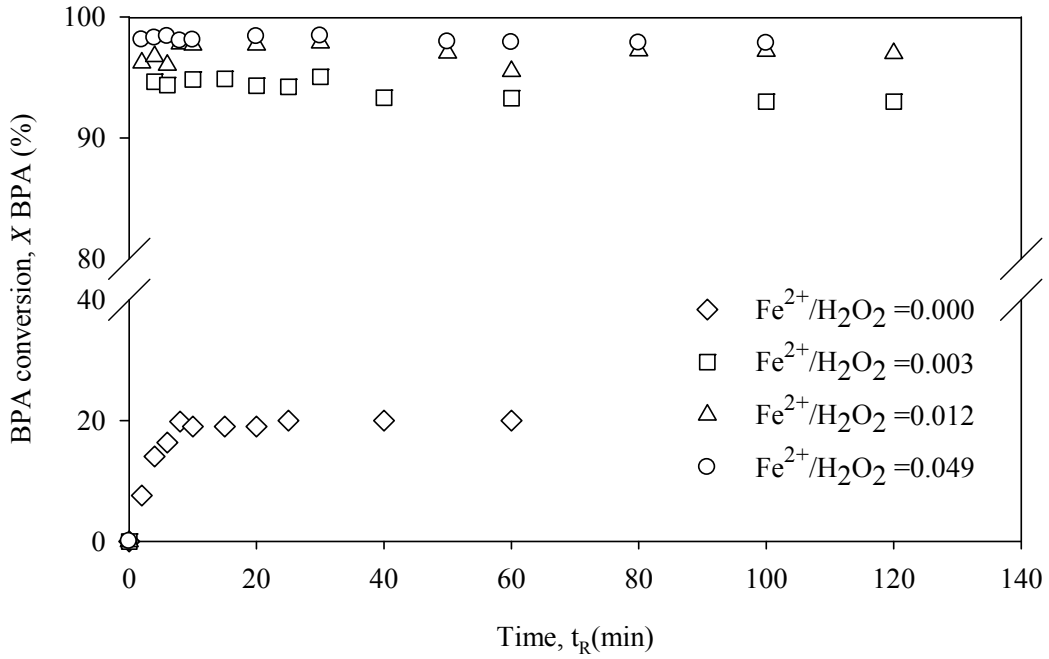

Figure 4. BPA conversion as a function of Fe^{+2}/H_2O_2 molar ratio. Conditions: [BPA] = 300 mg/L, H_2O_2/BPA = 0.20, pH_r = 3, T_r = 30 ^oC and 300 rpm.

The final pH (pH_f) of the oxidised effluent is also shown in Table 3. The uncontrolled pH slightly decreases along the reaction in all conditions tested. The highest decrease was observed in the evaluation of the effect of H_2O_2/BPA stoichiometric molar ratio, where the pH oscillates between 2.98 and 2.43 in the range from 0.05 to 1.00 of H_2O_2/BPA stoichiometric molar ratio, respectively. These pHs clearly suggest the formation of acidic species in the reaction medium. Torres et al [38] and Poerschmann et al [39] reported the formation of aromatic intermediates during oxidative degradation of BPA by Fenton. They detected a wide array of aromatic products in the molecular weight range between 94 Da (phenol) and 500 Da, including the occurrence of aromatic intermediates larger than BPA. 4-isopropenylphenol and 4-hydroxyacetophenone were the most abundant aromatic intermediates with molecular weights lower than BPA. Likewise, ring opening products, such as lactic, acetic and dicarboxylic acids, were also detected [38, 39]. Since some of those intermediates are recalcitrant, this poses a derived potential ecotoxicological risk. They should be carefully considered and, consequently, further research is required to optimize Fenton-driven remediation systems.

In addition, Table 3 collects the pre-oxidised absorbance of the effluents, spectrophotometrically measured at 400 nm of wavelength. This wavelength was selected

because it was stated that oxidised effluents showed a maximum in the absorbance spectrum at this value. The colour differences or absorbencies could be correlated with the formation of coloured aromatic intermediates.

3.2 BPA removal by nanofiltration membrane

The actual permeabilities of the tested NF membranes are shown in Table 2. The pure water permeabilities of the virgin NF membranes ranged from 1.56 to 14.4 (L/ h m^2 bar) at 30^{o}C. It can be seen that the permeabilities of the studied NF membranes increase in the following order: CK<NFD<ESNA<NF90<NF270. Since the materials and the membrane pore sides are in the same range for all membranes used, the differences in the pure water permeabilities could rather be related with differences in the membrane porosity and hydrophobicity. The contact angle water/membrane is an indicator for the overall hydrophobicity of a membrane. The permeability of the membranes decreased with increasing contact angle and thus hydrophobicity. Hence, CK membrane, which showed the lowest water permeability, was the most relatively hydrophobic membrane, as seen in Table 2, and might also be the less porous membrane.

Normalised fluxes and BPA rejection for membranes were measured using a feed solution consisting of 300 mg/L BPA, at 6 bar and 30 ºC (Figure 5). All the membranes depicted a typical permeate flux profile where the membrane is organically fouled. The normalised flux dropped by between 47 and 77% within the first minutes after the filtration start, and then the normalised flux remained in a nearly steady state. The normalised flux for ESNA presented the slowest decline, followed by NF90, NFD, NF270 and CK. The normalised flux decline can be due to a number of contributions such as concentration polarisation (CP), fouling that can be chemically reversed, and irreversible fouling, too. Figure 6 shows the normalised fluxes at the end of the filtration (after 200 min), J_p/J_{w0}, and also after flushing the used membrane with deionised water, J_{wf}/J_{w0}. The flux recovery after flushing the membranes with water is an indicator of the CP and reversible fouling contributions. The portion of the flux not recovered represents the irreversible flux decline (caused by fouling) and the reversible flux decline represents CP and/or reversible fouling, usually owing to adsorption phenomena. Since the reversible adsorption/desorption phenomena is a slower process than the immediate elimination of CP, the normalised permeate flux measured after immediate water flushing could also be a qualitative measure of CP. Figure 6 corroborates that both polarisation and

fouling actually occurred in all the membranes during the nanofiltration of BPA. In Figure 6, the concentration polarisation is assigned to the part of normalised flux recovered after immediate water flushing, and fouling to the part still not recovered.

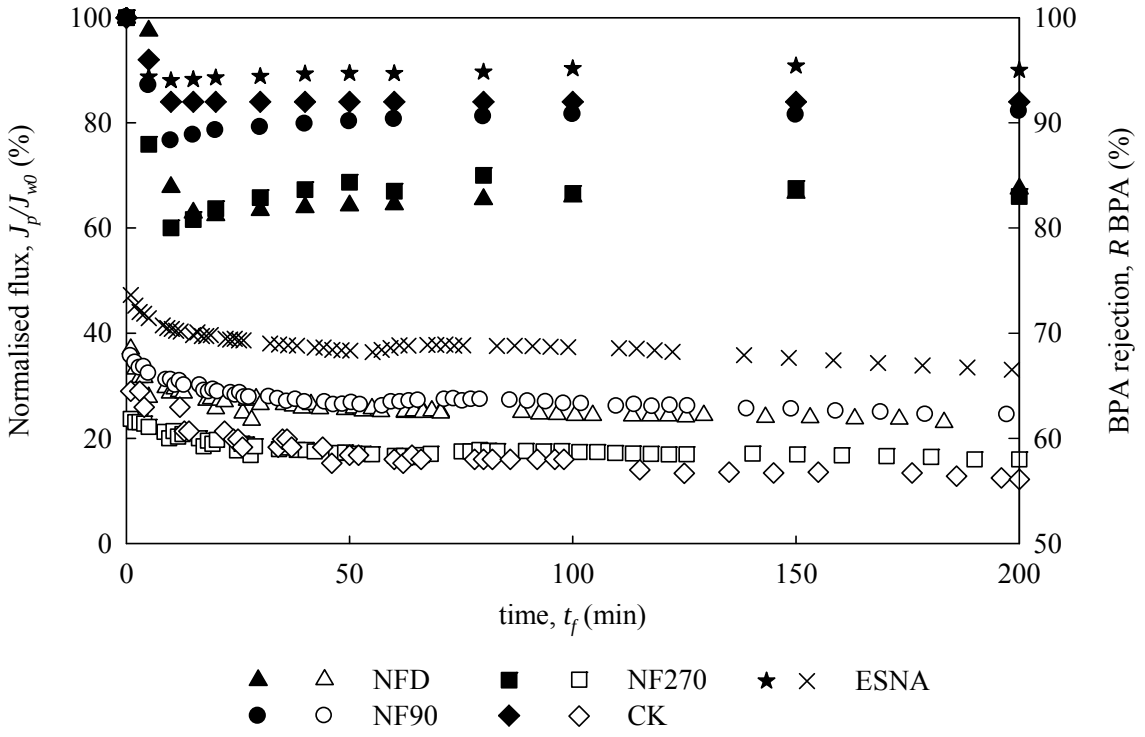

Figure 5. Normalised permeate flux and retention of bisphenol A as a function of NF time for several membranes. The feed solution contained 300 mg/L of BPA in deionised water. Experimental filtration conditions: TMP = 6 bar, Q_f = 20 L/h, pH_f = 6, and T_f = 30 ºC. Open symbols represent normalised flux and closed symbols BPA rejection.

The normalised flux drop by CP was always higher than the loss by fouling. Thus, CP (including very weakly adsorbed organics) was the main responsible of the normalised flux decline for all the studied membranes. Membrane fouling showed to increase in the following order: NFD<NF270<CK<NF90<ESNA. As BPA has similar size to the membrane pore, this suggests a fouling mechanism by pore blockage. However, in the evaluation of the membrane performance for rejection of hydrophobic compounds, such as BPA, the adsorption of the compound on the membrane has to be also taken into account. Hydrophobic compounds tend to strongly bind to hydrophobic materials. Hence, adsorption of organic compounds may be related to a change in hydrophobicity of the membrane surface, and could be an indicator to measure the fouling. By inspecting Figure 6 and Table 2 at once, it can be deducted that fouling increased as long as water contact angle did. Similar rapid flux decline as a result of

initial pore restriction and compound adsorption on the membrane surface have previously been elsewhere reported [40-42].

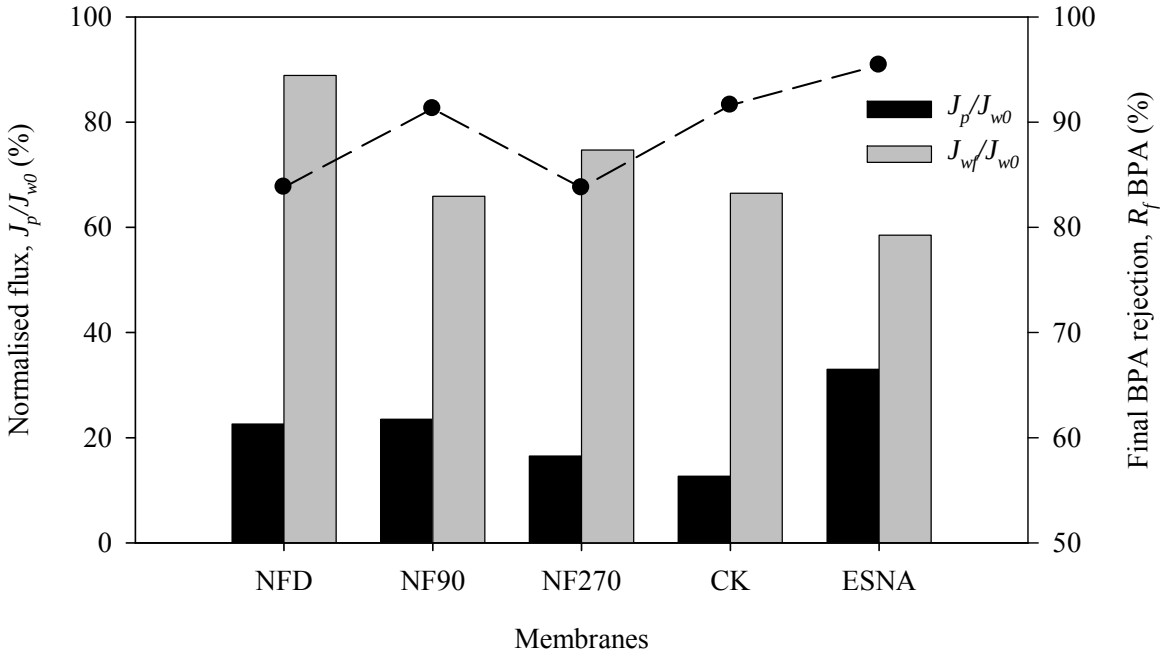

Figure 6. Normalised permeate flux at the end of bisphenol A NF, and BPA final rejection for several membranes. The feed solution contained 300 mg/L of BPA in deionised water. Experimental filtration conditions: TMP = 6 bar, Q_f = 20 L/h, pH = 6, and T_f = 30 ºC.

On the other hand, BPA rejection follows the same trends than membrane fouling. It apparently seems than an increase on membrane fouling enhanced the rejection. Thus, the driving mechanism for BPA rejection, besides including the BPA rejection by steric hindrance, probably is also related to the adsorption of BPA by hydrophobic–hydrophobic solute-membrane interactions. Past studies have reported that membrane fouling can both increase and decrease solute rejection depending on the solute, membrane, and foulant [41, 43, 44]. The rejection of trace organics is often explained by the solution diffusion model. According to this model, solute transportation across the membrane is a two-step process: first, the solute is adsorbed or dissolved by the membrane; second, it migrates across the membrane by diffusion or convection. This would mean that an increase in the BPA adsorption could facilitate transport by diffusion, resulting in a decrease of its rejection. Hypothetically, when the adsorption does not reach the equilibrium or saturation state, the membrane accumulates the solute and the rejection is overestimated. Thus, the observed BPA rejections could be slightly modify due to the adsorption of BPA by hydrophobic–hydrophobic solute-membrane interactions. The overestimation in the BPA rejection before

reaching equilibrium state in the BPA adsorption was already recorded by Xu et al. [42], who found that bromoform, which is more hydrophobic than chloroform, contributed to a higher initial removal; however, after approximately five hours of operation, rejection decreased significantly and levelled off between 20 and 35% for chloroform and 35 to 45% for bromoform, respectively.

The performance of NF90 membrane at different feed concentration is shown in Figure 7. Although ESNA membrane showed the lowest flow decay and highest BPA rejection, NF90 membrane was selected as the best membrane for BPA removal by NF, since NF90 membrane fouling was lower than ESNA. Thus, the examination of the effect of feed concentration was done using NF90. It is evident that the feed concentration had a negative effect on BPA nanofiltration. Normalised flux after 200 min of filtration decreased from 58.3 to 23.5% when the BPA feed concentration increased from 25 to 300 mg/L. As it expected, this decline in the normalised flux results from the increasing CP and fouling that lead to a loss in membrane performance. In Figure 8, it can be observed how these resistances increased as a function of the feed concentration, again considering, as it was above mentioned, CP as the portion of normalised flux recovered by water flushing, and the fouling as the portion lost.

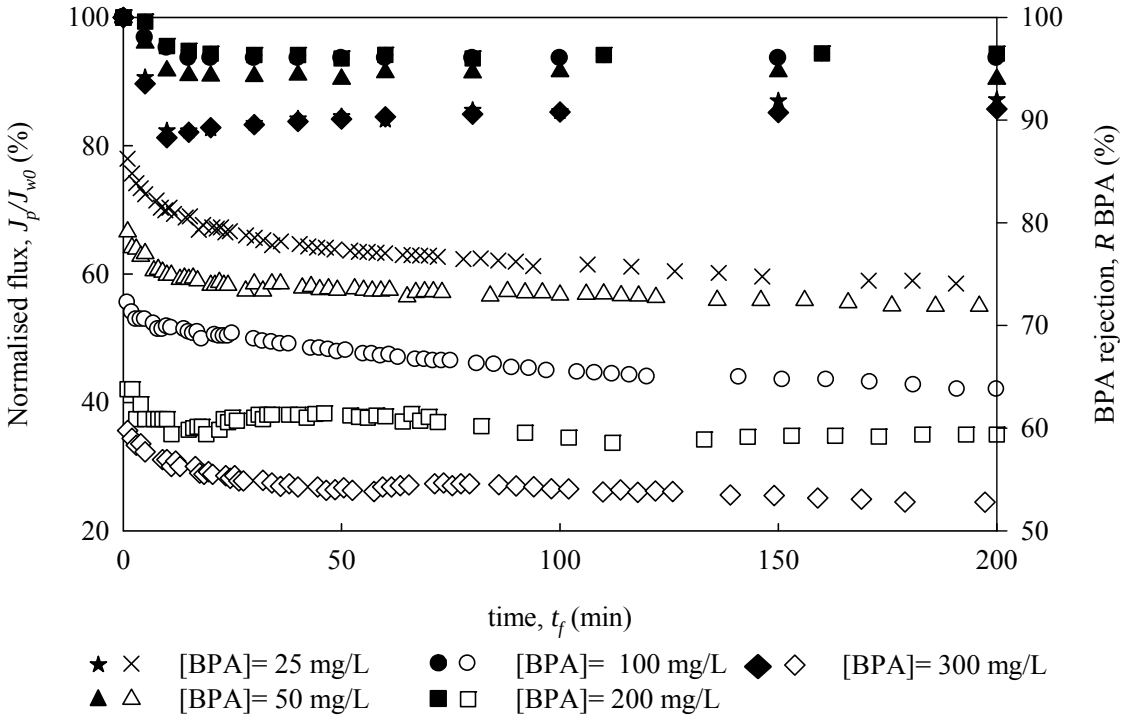

Figure 7. Normalised permeate flux as a function of NF time for several BPA feed concentrations. Experimental filtration conditions: membrane = NF90, Q_f = 20 L/h, pH = 6, and T_f = 30 ºC. Open symbols represent normalised flux and closed symbols BPA rejection.

Figure 8 also depict the final BPA rejection at 200 min of filtration for the different feed concentration tested. BPA rejection seems to have a maximum value at 100 mg/L of BPA. This retention behaviour by NF90 membrane can be ascribed to the adsorption/diffusion mechanism. At less than 100 mg/L of BPA concentration, much available sites for adsorption allowed membrane to adsorb more BPA, resulting in higher BPA removal. With the increase of BPA concentration, the membrane became closer to saturation, resulting in reduction in BPA removal as BPA accumulates on the membrane surface. The influence of the feed concentration on BPA rejection obtained in this study is somewhat inconsistent with some previous studies [24, 25], where the BPA rejection decreased with the increase of feed concentration. This may own to the high concentration used here or other different solution properties and different characteristics of membrane. However, similar behaviour has also been reported by Bing-zhi et al. [45] in the removal of BPA by hollow fibre microfiltration membrane.

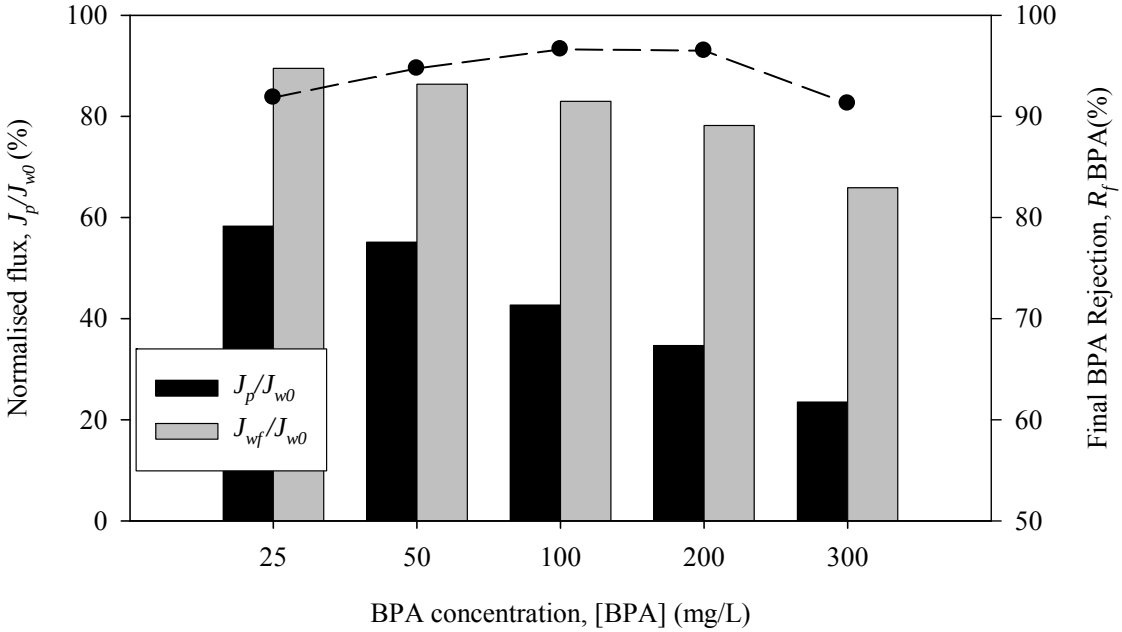

Figure 8. Normalised permeate flux at the end bisphenol NF, and BPA final rejection for the several BPA concentrations. Experimental filtration conditions: membrane = NF90, Q_f = 20 L/h, pH = 6, and T_f = 30 ºC.

3.3 Removal of BPA effluent after Fenton oxidation by nanofiltration membrane

In this set of NF experiments, the feed solution was the final effluent after Fenton treatment in the optimal conditions selected ($[BPA]_0$ = 300 mg/L, H_2O_2/BPA = 0.20 and Fe^{2+}/BPA = 0.012). The Fenton treated effluent contained 571 ± 50 mg/L of COD, 222 ± 20 mg/L of TOC, pH = 2.71 ± 0.04 and an absorbance of 0.6508 ± 0.0002 recorded at 400 nm. Figure 9 represents the normalized flux of permeate for the studied membranes as a function of time for this Fenton treated effluent. In general, the flux strongly fell during the first period of filtration, e.g., the flux was 40% of the original pure water flux after 25 minutes of filtration for NF90 membrane. Afterwards, the flux declined more gradually until, in some cases, a quasi-steady state value was obtained after approximately 200 minutes. The patterns of flux decline varied between the membranes in the membrane screening study. As it can be seen from Figure 9, the CK membrane featured the lowest permeate flux decay at 6 bar, followed by NFD, NF270 and ESNA with closely flux decays, and finally by NF90 with the highest flux fall. These trends are connected to an increase of the resistance to the pass through the membrane, which could result from either CP, adsorption of solutes on the membrane, gel formation, internal pore fouling (pore blocking) and external deposition or cake formation.

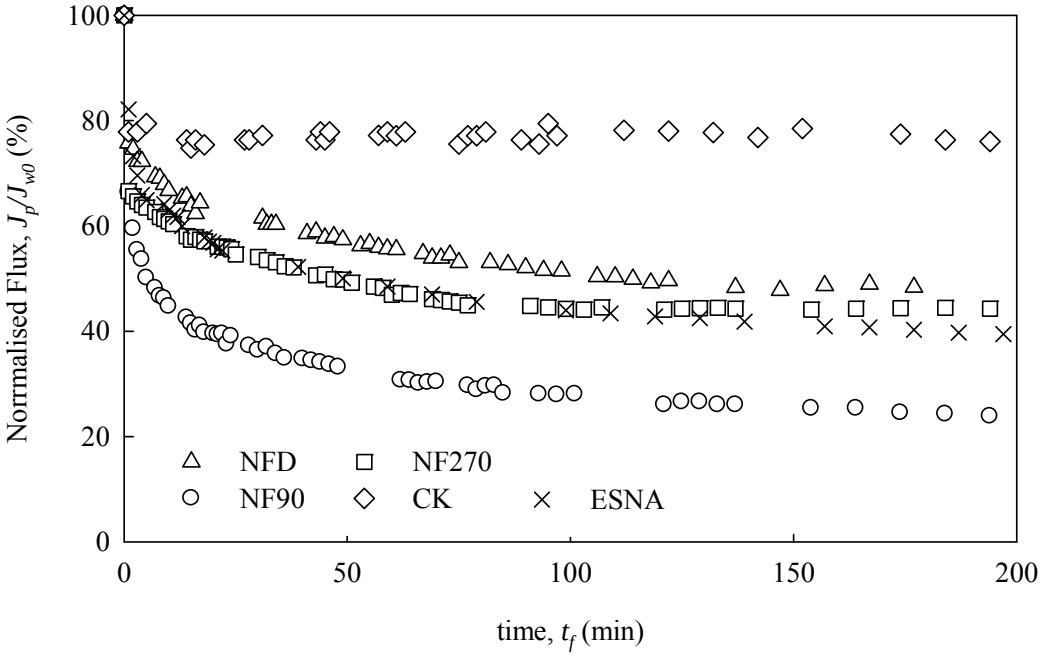

Figure 9. Normalised permeate flux as a function of time for several membranes in the NF of Fenton treated effluent. Experimental filtration conditions: Q_f = 20 L/h, pH = 3, and T_f = 30 ºC.

Figure 10 proved that in the NF of Fenton effluent, membrane fouling plays a predominant role in the loss of flux. As it can be seen, after flushing the membranes with water, the

normalised permeate fluxes were only recovered as much as 14% of the maximum flux decay experienced by each membrane. Excluding NF270 membrane, the membrane fouling seemed to be related with the membrane pore size and pK_a. Based on pure water permabilities and MWCO of the studied membranes, it could be expected that the pore size follows the same trend. Depending on the ratio between the solute size and the pore diameter of the membrane, the different types of fouling can occur. If the pores are very small in comparison to the solute diameter, the formation of a cake layer is favoured. If the pores are greater than the solute diameter, complete and/or partial pore blocking can occur. In this study, the fouling increased with the membrane pore size. Anyway, the specific predominating type of fouling could be difficult to distinguish, since it would require the detailed characterization of the Fenton treated effluent. The only fouling that could be confirmed was the formation of a cake layer, which was visually observed at the end of each experiment, as a dark brown layer of organic materials firmly attached to the membrane surface.

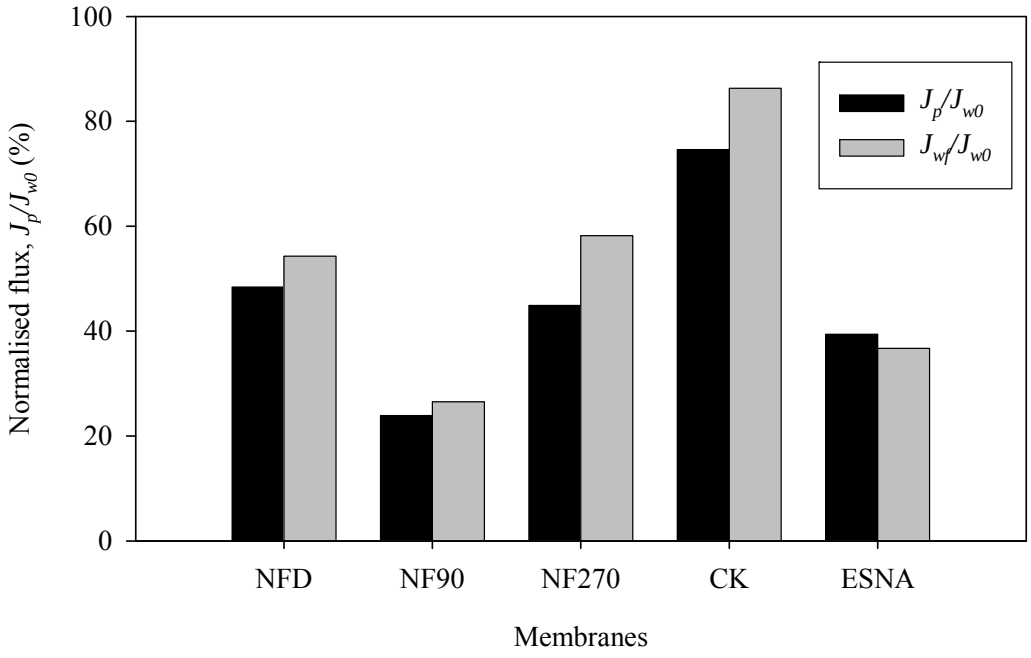

Figure 10. Normalised permeate flux at the end of Fenton treated effluent NF for several membranes. Experimental filtration conditions: Q_f = 20 L/h, pH = 3, and T_f = 30 ºC.

The sieving features of a NF membrane are important for the separation of uncharged molecules; however, in the case of ions, both sieving features and electrostatic repulsion between the charged membrane and the solute may become important. The production of species positively charged during Fenton oxidation at pH around 3 could facilitate their rejection by repulsion between the positively charged membrane and the solutes, which

decreased the probability of fouling. Regarding Table 2 and Figure 10, one can observe that the fouling is reduced for more positively charged membrane.

The final normalised flux decay for NF of Fenton effluents was generally lower compared to the NF of BPA alone. From Figure 6 and 10, it can be found that the final normalised permeate fluxes are 25.3, 28.0, 61.9 and 3.37% higher for NFD, NF270, CK and ESNA, respectively. In contrast, the normalised flux after flushing was generally lower, which suggest a major contribution of irreversible fouling in the presence of oxidation products and a very different pattern of interactions between the organic products and the membrane.

The flux decay at different pressures was also studied, although not shown here. Four operating pressures (2, 4, 6 and 8 bar) were applied during the NF of BPA effluent after Fenton degradation using NF270 membrane. The results indicate that the increase of the operating pressure provided a negative effect on the performance of NF270 membrane. In general, an increase in the transmembrane pressure should result in an increase in the permeate flux, but this behaviour was not observed in this case. The normalised flow decays more quietly when the transmembrane pressure increases. If the increase in fouling rate is much higher than the increase in permeate flux, the permeate flux can even decline at higher transmembrane pressure due to the compaction of the cake [46]. Thus, low operating pressures here seems to diminish membrane flux decline by decreasing the permeation drag through the membrane, and consequently the contact between the fouling layer and the membrane surface.

In general, the rejection of COD, TOC, colour and Fe^{2+} in the NF of Fenton treated effluent were always higher than 81% (Table 4). This behaviour can be related to the classical molecular size exclusion and the formation of a fouling layer.

Table 4. Rejection of COD, TOC, colour and Fe^{2+} in the NF of Fenton effluent for several membranes. Experimental filtration conditions: Q_f = 20 L/h, pH = 3, and T_f = 30 ºC.

Membrane name	R_{COD} (%)	R_{COT} (%)	R_{Colour} (%)	R_{Fe2+} (%)
NFD	88.3 ± 1.3	87.5 ± 0.8	93.2 ± 1.3	81.9 ± 1.9
NF90	84.0 ± 2.8	76.5 ± 0.5	97.7 ± 1.1	96.2 ± 0.3
NF270	97.7 ± 0.2	88.9 ± 0.1	95.5 ± 1.4	92.4 ± 0.2
CK	100.0 ± 2.0	91.9 ± 0.7	100.0 ± 2.7	91.10 ± 0.01
ESNA	85.1 ± 2.1	82.2 ± 0.1	94.2 ± 0.7	97.7 ± 0.4

4. CONCLUSIONS

The degradation of BPA in aqueous solution by Fenton process was investigated under various operating conditions. The experimental results indicate that BPA could be efficiently degraded by Fenton treatment in the ranges studied, resulting in almost full BPA conversion, and 78.2 and 59.1% for COD and TOC conversions, respectively. These values were obtained using just the stoichiometric H_2O_2/BPA molar ratio and pH 3. The removal efficiencies of BPA, TOC and COD were hindered by excess H_2O_2 (H_2O_2/BPA≥1.12) due to scavenging of the hydroxyl radicals usable in the process due to the competence of the partially oxidised compounds resulting from the higher mineralisation.

The NF of BPA shows the general ability of membrane processes to contribute significantly to the removal of organics in wastewater treatment. A BPA rejection over 80% was obtained by all the used membranes. The BPA removal was attributed to size exclusion as well as BPA adsorption on membrane, which was related with the membrane hydrophobicity. Normalised flux decline in the NF of BPA was strongly affected by concentration polarisation phenomena. This was corroborated with the high permeate flux recovery after membrane flushing with water.

Overall, coupling of Fenton process and NF allows total BPA abatement by Fenton process. In addition, over 77% in COD, TOC, colour and Fe^{2+} rejections were achieved by NF, which suggests that recirculation is possible for increasing mineralisation and saving of iron salts. Poorer permeation performance in NF of Fenton treated effluent shows to be mainly related

with membrane fouling ascribed to the derived partially oxidised products, although it is still within typical values in membrane operation.

Acknowledgements

Financial support for this research was provided by the Spanish Ministerio de Educación y Ciencia and FEDER (grants CTM2008-03338 and CTM2011-23069). The Generalitat de Catalunya and the European Social Fund are also thanked for providing a doctoral scholarship to carry out this research work. The author's research group is recognised by the Comissionat per a Universitats i Recerca del DIUE de la Generalitat de Catalunya (2009SGR865) and supported by the Universitat Rovira i Virgili (2010PFR-URV-B2-41).

References

[1] Sonnenschein, C. and A. Soto (1998). "An updated review of environmental estrogens and androgen mimics and antagonists." Journal of Steroid Biochemistry and molecular biology 65(1-6): 143–150.

[2] Mendes, A. (2002). "The endocrine disrupters: a major medical challenge." Food and Chemical Toxicoogy 40(6): 781–788.

[3] Wetherill, Y., B. Akingbemi, J. Kanno, J. McLachlan, A. Nadal, C. Sonnenschein, C. Watson, R. Thomas Zoeller and S. Belcher (2007). "In vitro molecular mechanisms of bisphenol. A action." Reproductive Toxicology 24(2): 178–198.

[4] Flint, S., T. Markle, S. Thompson and E. Wallace (2012). "Bisphenol A exposure, effects, and policy: A wildlife perspective." Journal of Environmental Management 104: 19-34.

[5] Yamamoto, T., A. Yasuhara, H. Shiraishi and O. Nakasugi (2001). "Bisphenol A in hazardous waste landfill leachates." Chemosphere 42(4): 415–418.

[6] Kolpin, D., E. Furlong, M. Meyer, E. Thurman, S. Zaugg, L. Barber and H. Buxton (2002). "Pharmaceuticals, hormones, and other organic wastewater contaminants in U.S.

streams, 1999–2000: a national reconnaissance.” Environmental Science and Technoogy 36(6): 1202–1211.

[7] Ministry of Health, Labour and Welfare of Japan (Eds.), Exposure and behaviour researches of endocrine disrupting chemicals in tap water. Japan, 2000.

[8] Fürhacker, M., Scharf, S., Weber, H. (2000). “Bisphenol A: emissions from point sources” Chemosphere 41(5): 751-756

[9] Kaiser, J. (2000). “Panel cautiously confirms low-dose effects.” Science 290(1): 695–697.

[10] Samuelsen, M., C. Olsen and J. Holme (2001). “Estrogen-like properties of brominated analogs of bisphenol-A in the MCF-7 human breast cancer cell line.” Cell Biolgy and Toxicology 17(3): 139–151.

[11] Chang, H., K. Choo, B. Lee and S. Choi (2009). “The methods of identification, analysis, and removal of endocrine disrupting compounds (EDCs) in water.” Journal of Hazardous Materials 172(1): 1–12.

[12] Staples, C.A., P. Dom, G. Klecka, S. O’Block and L. Harris (1998). “A review of the environment fate, effects, and exposures of bisphenol A.” Chemosphere 36(10): 2149–2173.

[13] Kang, J. and F. Kondo (2002). “Bisphenol a degradation by bacteria isolated from river water.” Archives of Environmental Contamination Toxicology 43: 265–269.

[14] Xuan, Y., Y. Endo and K. Fujimoto (2002). “Oxidative degradation of bisphenol a by crude enzyme prepared from potato.” Journal of Agricultural and Food Chemistry 50(22): 6575–6578.

[15] Kuramitz, H., M. Matsushita and S.Tanaka (2004). “Electrochemical removal of bisphenol A based on the anodic polymerization using a column type carbon fiber electrode.” Water Research 38(9): 2331–2338.

[16] Wang, R., D. Ren, S. Xia, Y. Zhang and J. Zhao (2009). "Photocatalytic degradation of BPA using immobilized TiO_2 and UV illumination in a horizontal circulating bed photocatalytic reactor." Journal of Hazardous Materials 169(1-3): 926–932.

[17] Fukahori, S., H. Ichiura, T. Kitaoka and H. Tanaka (2003). "Capturing of bisphenol A photodecomposition intermediates by composite TiO_2-zeolite sheets." Applied Catalysis B: Environmental 46(3): 453–462.

[18] Garoma, T. and S. Matsumoto (2009). "Ozonation of aqueous solution containing bisphenol A: Effect of operational parameters." Journal of Hazardous Materials 167(1-3): 1185–1191.

[19] Chen, P, K. Linden, D. Hinton, S. Kashiwada, E. Rosenfeldt and S. Kullman (2006). "Biological assessment of bisphenol A degradation in water following direct photolysis and UV advanced oxidation." Chemosphere 65(7): 1094–1102.

[20] Rosenfeldt, E. and K. Linden (2004). "Degradation of endocrine disrupting chemicals BPA, ethinyl estradiol, and estradiol during UV photolysis and AOP." Environmental Science and Technology 38(20): 5476–5483.

[21] Katsumata, H., S. Kawabe, S. Kaneco, T. Suzuki and O. Kiyohisa (2004). "Degradation of bisphenol A in water by the photo-Fenton reaction." Journal of Photochemistry and Photobiology A: Chemistry 162(2-3): 297–305.

[22] Walling , C. and S. Kato (1971). "Oxidation of alcohols by Fenton's reagent. Effect of copper ion." Journal of the American Chemical Society 93(17): 4275–4281.

[23] Rautenbach, R. and R. Mellis (1995). "Hybrid processes involving membranes for the treatment of highly organic/inorganic contaminated waste water." Desalination 101(2): 105-113.

[24] Zhang, Y., C. Causserand, P. Aimar and J. Cravedi (2006). "Removal of bisphenol A by a nanofiltration membrane in view of drinking water production." Water Research 40(20):3793–3799.

[25] Su-Hua, W., D. Bing-zhi and H. Yu (2010). “Adsorption of bisphenol A by polysulphone membrane.” Desalination 253(1-3): 22–29.

[26] Tanninen, J., M. Mänttäri and M. Nyström (2006). “Effect of salt mixture concentration on fractionation with NF membranes.” Journal of Membrane Science 283(1–2): 57-64.

[27] Balannec, B., M. Vourch, M. Rabiller-Baudry and B. Chaufe (2005). “Comparative study of different nanofiltration and reverse osmosis membranes for dairy effluent treatment by dead-end filtration.” Separation and Purification Technology 42(2): 195-200.

[28] Nghiem, L.D., Removal of emerging trace organic contaminants by nanofiltration and reverse osmosis, in: School of Civil Mining and Environmental Engineering, University of Wollongong, Wollongong, 2005.

[29] Liikanen, R., Nanofiltration as a refining phase in surface water treatment, in: Laboratory of Water and Wastewater Engineering, Helsinki University of Technology, Helsinki, 2006.

[30] Benitez, F., J. Acero, F. Real and C. Garcia (2009). “Removal of phenyl-urea herbicides in ultrapure water by ultrafiltration and nanofiltration processes.” Water Research 43(2): 267-276.

[31] Negaresh, E., A. Antony, M. Bassandeh, D. Richardson and G. Leslie (2012). “Selective separation of contaminants from paper mill effluent using nanofiltration.” Chemical Engineering Research and Design 90(4): 576–583.

[32] Pignatello, J., E. Oliveros and A. MacKay (2006). “Advanced Oxidation Processes for organic contaminant destruction based on the Fenton reaction and related chemistry.” Critical Reviews in Environmental Science and Technology 36(1):1-84.

[33] Guedes, A., L. Madeira, R. Boaventura and C. Costa (2003). “Fenton oxidation of cork cooking wastewater-overall kinetic analysis.” Water Research 37(13): 3061-3069.

[34] Kang, Y., M. Cho and K. Hwang (1999). “Correction of hydrogen peroxide interference on standard chemical oxygen demand test.” Water Research 33(5): 1247-1251.

[35] Clesceri, L.S. et al., Standard Methods for the Examination of Water and Wastewater, 17th edition, American Public Health Association and American Water Works Association, Washington, USA, 1989.

[36] Poerschmann, J., U. Trommler and T. Górecki (2010). “Aromatic intermediate formation during oxidative degradation of Bisphenol A by homogeneous sub-stoichiometric Fenton reaction.” Chemosphere 79(10): 975–986.

[37] Tang, W. and C. Huang (1997). “Stoichiometry of Fenton’s reagent in the oxidation of chlorinated organic pollutants.” Environmental Science and Technology 18:13–23.

[38] Torres, R., F. Abdelmalek, E. Combet, C. Pétrier and C. Pulgarin (2007). “A comparative study of ultrasonic cavitation and Fenton's reagent for bisphenol A degradation in deionised and natural waters.” Journal of Hazardous Materials 46(3): 546-551.

[39] Poerschmann, J., U. Trommler and T. Góreck (2010). “Aromatic intermediate formation during oxidative degradation of Bisphenol A by homogeneous sub-stoichiometric Fenton reaction.” Chemosphere 79(10): 975-986.

[40] Van der Bruggen, B. and C. Vandecasteele (2001). “Flux decline during nanofiltration of organic components in aqueous solution.” Environmental Science and Technology 35(17): 3535–3540.

[41] Nghiem, L. and S. Hawkes (2007). “Effects of membrane fouling on the nanofiltration of pharmaceutically active compounds (PhACs): Mechanisms and role of membrane pore size.” Separation and Purification Technology 57(1): 176-184.

[42] Xu, P., J. Drewes, C. Bellona, G. Amy, T. Kim, M. Adam and T. Heberer (2005). “Rejection of Emerging Organic Micropollutants in Nanofiltration–Reverse Osmosis Membrane Applications.” Water Environment Research 77(1): 40-48.

[43] Bellona, C., M. Marts and J. Drewes (2010). “The effect of organic membrane fouling on the properties and rejection characteristics of nanofiltration membranes.” Separation and Purification Technology 74(1): 44–54.

[44] Comerton, A., R. Andrews, D. Bagley and C. Hao (2008). “The rejection of endocrine disrupting and pharmaceutically active compounds by NF and RO membranes as a function of compound and water matrix properties.” Journal of Membrane Science 313(1-2): 323-335

[45] Bing-zhi, D., C. Hua-qiang, W. Lin, X. Sheng-ji and G. Nai-yun (2010). “The removal of bisphenol A by hollow fiber microfiltration membrane.” Desalination 250(2): 693–697

[46] Seidel, A. and M. Elimelech (2002). “Coupling between chemical and physical interactions in NOM fouling of nanofiltration membranes: implications for fouling control.” Journal of Membrane Science 203(12): 245-255.